Online Supplementary Information for

Three-dimensional Polymer Constructs Exhibiting a Tunable Negative Poisson's Ratio

David Y. Fozdar[1], Pranav Soman[1*], Jin Woo Lee[1], Li-Hsin Han[2], Shaochen Chen[1†]*

[1]Department of NanoEngineering, University of California, San Diego
9500 Gilman Drive, Atkinson Hall, MC-0448, La Jolla, CA 92093

[2](present address) Department of Orthopaedic Surgery, Stanford University School of Medicine, 300 Pasteur Dr., Edwards R132, Stanford, CA 94305

*These authors contributed equally to this work.

[†]To whom correspondence should be addressed. Email: chen168@ucsd.edu.

Supplementary Information:

Supplementary Discussions 1 and 2
Supplementary Figures 1 and 2
References for Supplementary Information
Captions for Supplementary Movies 1-6

Supplementary Discussion 1: Calculation of Poisson's Ratios

To calculate Poisson's ratios, we evaluated the overall transverse elastic deformation of the scaffolds resulting from axial strains. We determined Poisson's ratios using equation 1 *[42]*.

$$\upsilon_{xy} = -\frac{\varepsilon_y}{\varepsilon_x} \qquad (1)$$

where ε_y is transverse strain resulting from an axial strain ε_x. The subscripts *x* and *y* denote the axial and transverse strain directions, respectively, in a two-dimensional Cartesian coordinate system with orthogonal x- and y-axes. We note that we calculated in-plane values of Poisson's ratio resulting from in-plane strains. Poisson's ratio was determined from values of true strain. Total true strain, ε_i, was calculated by equation (2) (for any in-plane coordinate direction).

$$\varepsilon_i = \ln\left(\frac{L_i}{L_0}\right) = \sum_i \left[\ln\left(\frac{L_i}{L_{i-1}}\right) + \varepsilon_{i-1}\right] \qquad (2)$$

where $i = 1, 2, 3, ..., n$ and denotes the current strain state, L_1 is the current specimen length for strain state i, and L_0 is the initial undeformed specimen length. Total true strain was determined by summing contributions to total true strain from the application of incremental true strains. True strain was used in our calculations of Poisson's ratio, as opposed to engineering strain, due to the magnitudes of the strains involved in our experiments.

Supplementary Discussion 2: Unit-cell analytical models

To determine how precisely we could tune the strain-dependent Poisson's ratios of our 3D PEG constructs, we compared our experimental strain data with analytical models reported in

the literature. The analytical models described here contain parameters that are shown in Figure 1B in the main text. We determined the Poisson's ratios of the biomaterial constructs by measuring the overall strains in the x- and y-directions and did not measure changes in the internal angles of the unit-cells. To determine the deformed values of the internal angles of the unit-cells, we used our empirically-obtained values of axial strain in analytical equations relating axial strain to the deformed values of the internal angles [Note: unless otherwise noted, all angle values have units of degrees]. The strain-angle relations for the missing and intact rib structures include constants that constrain the relations so that they yield zero axial strain for the undeformed values of the angles. The constants were determined by stipulating the initial condition that axial strain was zero for the undeformed values of the internal angles. The equations, relating axial strain to the deformed values of the internal angles in the unit-cells, were used to plot the analytical models as a function of axial strain. This made it possible to directly compare the strain-dependent rates of change of Poisson's ratio between our experimental data and the analytical functions.

For the reentrant unit-cell, we compared our strain-dependent Poisson's ratio data with the hinging model [equation (3)] reported by Gibson and Ashby *[2]*. The model assumes a change in Poisson's ratio due solely to changes in angle ζ for a given set of rib lengths L_1 and L_2 (Figure 1B in main text). Because the strain-dependent Poisson's ratio of the reentrant hinging model is presented as a function of angle ζ, which changes as the unit-cell is axially strained, equation (4) was utilized to convert values of axial strain into deformed values of angle ζ *[43]*.

$$\upsilon_{xy} = \frac{\sin\zeta^*\left(L_2/L_1 + \sin\zeta^*\right)}{\cos^2\zeta^*} \quad (3)$$

$$\varepsilon_x = \ln\left(\frac{\cos\zeta^*}{\cos\zeta_0^*}\right) \qquad (4)$$

where $\zeta^* = 90^\circ - \zeta$. The subscript "0", represents the initial undeformed value of the angle (and does so hereafter). Figure 2 plots Poisson's ratio as a function of true strain given by equation (3), based on the undeformed dimensions of Figure 1B (main text).

For the missing rib model, we compared our data to the models reported by Smith et al. *[39]* and Gaspar et al. *[38]*, which are shown in equations (5) and (6), respectively. The angles in the equations are based on Figure 1B (main text).

$$\upsilon_{xy} = -\tan(\beta)\tan(\alpha_0^* - \beta) \qquad (5)$$

$$\upsilon_{xy} = -\frac{\left\{\cos\left[\alpha_0^* - \beta_0 + \Delta\beta(\kappa - 1)\right] - \cos(\alpha_0^* - \beta_0)\right\}\sin\beta_0}{(\sin\beta - \sin\beta_0)\cos(\alpha_0^* - \beta_0)} \qquad (6)$$

where $\alpha^* = 180^\circ - \alpha$ (Figure 1B in main text) and $\kappa = \Delta\alpha^*/\Delta\beta$ in the Gaspar model, which represents hinging at the central node [equation (6)]. A few differences exist between analytical models (5) and (6). While equation (5) was derived from true (instantaneous) strain considerations, equation (6) was formulated from engineering strain, an approximation usually reserved for small strains. Also, equation (5) assumes that only rotation occurs at the central node and excludes any hinging of the internal angle α (see Figure 1B in main text), i.e., $\Delta\alpha = 0$, which causes Poisson's ratio to remain constant (not strain-dependent) despite a change in angle β. On the other hand, equation (6) includes some hinging at the central node so that $|\Delta\alpha| \geq 0$. Our data for Poisson's ratio matched up well with the Gaspar model given our unit-cell dimensions, which shows that some hinging likely occurs when the missing rib structure is

axially strained. supplementary equation (7) relates axial strain with deformed values of angle β *[38, 39]*.

$$\varepsilon_{\mathrm{x}} = \ln\left|\sin\beta\right| + \mathrm{C} \qquad (7)$$

$$\text{where } \mathrm{C} = -\ln\left|\sin\beta_0\right| = 0.347\Big|_{\beta=45^\circ}.$$

In equation (7), constant *C* depends on the undeformed value of β. The constant enforces the initial condition that the axial strain is zero for the undeformed value of the angle, which was 45° for our missing rib design (Figure 1B in main text). Figure 2 plots Poisson's ratio as a function of engineering strain given by equation (6), based on the undeformed dimensions of Figure 1B (main text). For the intact rib model, we compared our strain data with the model proposed by Smith et al. *[39]*, which is shown in equations (8) and (9).

$$\upsilon_{\mathrm{xy}} = \tan^2\left(\frac{\gamma^*}{2}\right) \qquad (8)$$

$$\varepsilon_{\mathrm{x}} = \ln\left|\sin\left(\frac{\gamma^*}{2}\right)\right| + \mathrm{C} \qquad (9)$$

$$\text{where } \mathrm{C} = -\ln\left|\sin\left(\frac{\gamma_0^*}{2}\right)\right| = 0.347\Big|_{\gamma=90^\circ}.$$

where $\gamma^* = 180^\circ - \gamma$. In equation (9), constant *C* depends on the undeformed value of angle γ. The constant constrains equation (9) so that it yields a zero axial strain when γ equals its undeformed value, which was 90° for our structures (Figure 1B in main text). Figure 2 plots Poisson's ratio as a function of true strain given by equation (8), based on the undeformed dimensions of Figure 1B (main text).

References for online supplementary information:

1. Eisenstadt, M.M. *Introduction to mechanical properties of materials*, 1st Ed., (Macmillan, New York, NY, 1971), pp. 444.
2. Gibson, L.J., Ashby, M.F. *Cellular solids: structure and properties*, 2nd Ed., (Cambridge University Press, Cambridge, UK, 1997), pp. 510.
3. Alderson, A. *et al.* An auxetic filter: a tuneable filter displaying enhanced size selectivity or defouling properties, *Ind. Eng. Chem. Res.* **39**, 654 (2000).
4. Smith, C.W., Grima, J.N., Evans, K.E. A novel mechanism for generating auxetic behaviour in reticulated foams: missing rib foam model, *Acta Mater.* **48**, 4349 (2000).
5. Gaspar, N., Ren, X.J., Smith, C.W., Grima, J.N., Evans, K.E. Novel honeycombs with auxetic behaviour, *Acta Mater.* **53**, 2439 (2005).

Supplementary Figure Captions:

Figure 1. Schematic of the Digital Micromirror Device (DMD) apparatus used for fabricating 3D porous biomaterial constructs having tunable negative Poisson's ratios.

Figure 2. Poisson's ratio as a function of true strain given by the reentrant [equation (3)], missing rib [equation (6)] and intact rib [equation (8)] models *[2, 38, 39]*. The plots are based on the undeformed dimensions shown in Figure 1B in the main text.

Supplementary Movie Captions:

Movie 1: Simultaneous axial and transverse expansions of a single-layer PEG construct composed of the reentrant honeycomb unit-cell lattice. The construct exhibits a negative Poisson's ratio.

Movie 2: Simultaneous axial and transverse expansions of a single-layer PEG construct composed of the missing rib unit-cell lattice. The construct exhibits a negative Poisson's ratio.

Movie 3: Axial expansion but transverse compression of a single-layer PEG construct composed of the intact rib unit-cell lattice. The construct exhibits a large positive Poisson's ratio (used as a control in our tests for Poisson's ratio).

Movie 4: Simultaneous axial and transverse expansions of a two-layer PEG construct composed of the reentrant honeycomb unit-cell lattice. The cellular layers were stacked on top of one other with precise alignment by an alternating layer of vertical posts. The construct exhibits a negative Poisson's ratio similar in magnitude to the single-layer construct.

Movie 5: Simultaneous axial and transverse expansions of a two-layer PEG construct composed of the missing rib unit-cell lattice. The cellular layers were stacked on top of one other with precise alignment by an alternating layer of vertical posts. The construct exhibits a negative Poisson's ratio similar in magnitude to the single-layer construct.

Movie 6: Axial expansion but transverse compression of a two-layer PEG construct composed of the intact rib unit-cell lattice. The cellular layers were stacked on top of one other with precise alignment by an alternating layer of vertical posts. The construct exhibits a large positive Poisson's ratio similar in magnitude to the single-layer construct (used as a control in our tests for Poisson's ratio).

Supplementary Figure 1:

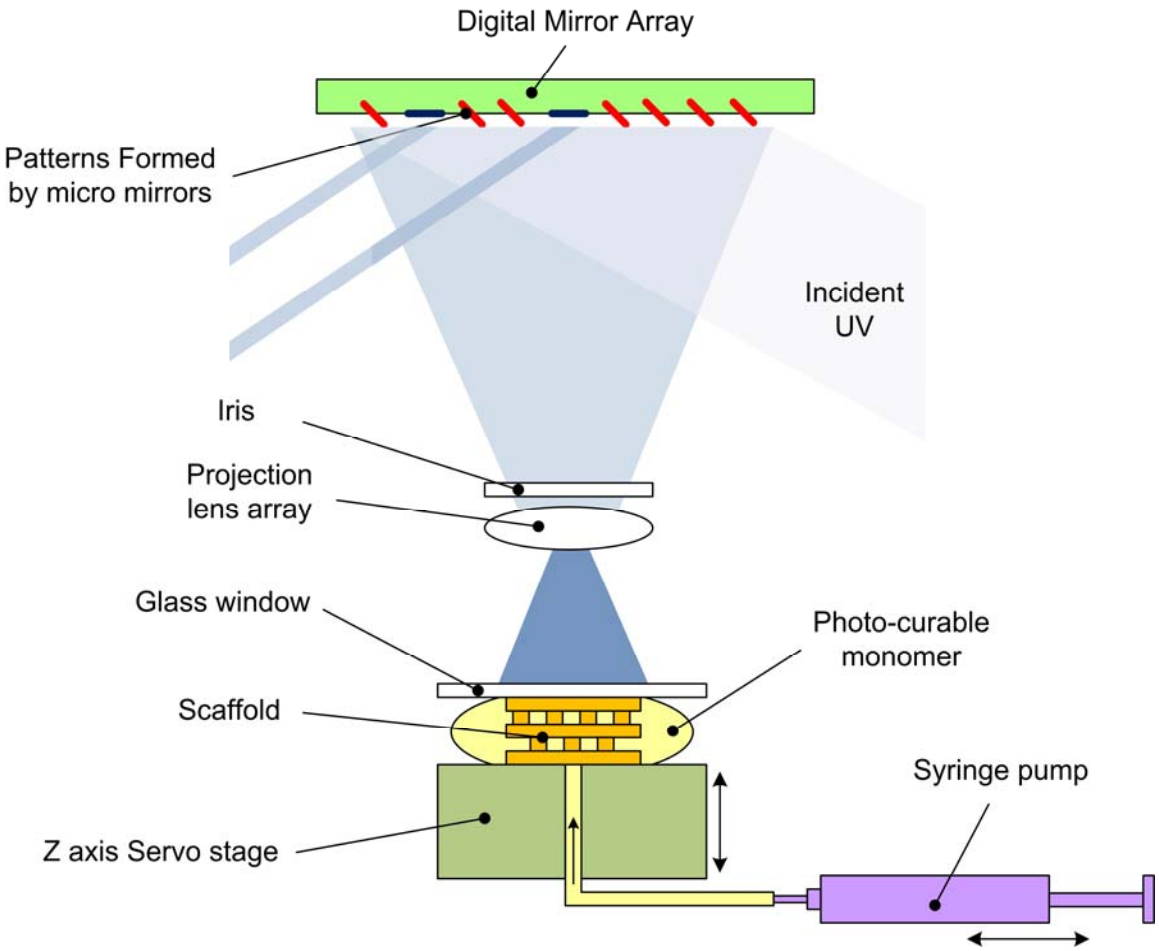

Supplementary Figure 2: